JACS
JOURNAL OF THE AMERICAN CHEMICAL SOCIETY
pubs.acs.org/JACS
Article

Reductive NO Coupling at Dicopper Center via a $[Cu_2(NO)_2]^{2+}$ Diamond-Core Intermediate

Wenjie Tao, Samantha Carter, Regina Trevino, Weiyao Zhang, Hannah S. Shafaat,* and Shiyu Zhang*

Cite This: https://doi.org/10.1021/jacs.2c09523
Read Online
ACCESS | Metrics & More | Article Recommendations | Supporting Information

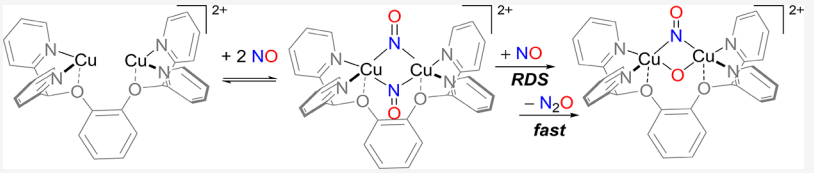

ABSTRACT: Treatment of a dicopper(I,I) complex with excess amounts of NO leads to the formation of a dicopper dinitrosyl $[Cu_2(NO)_2]^{2+}$ complex capable of (i) releasing two equivalents of NO reversibly in 90% yield and (ii) reacting with another equivalent of NO to afford N_2O and dicopper nitrosyl oxo species $[Cu_2(NO)(O)]^{2+}$. Resonance Raman characterization of the $[Cu_2(NO)_2]^{2+}$ complex shows a ^{15}N-sensitive N=O stretch at 1527.6 cm^{-1} and two Cu–N stretches at 390.6 and 414.1 cm^{-1}, supporting a symmetric diamond-core structure with bis-μ-NO ligands. The conversion of $[Cu_2(NO)_2]^{2+}$ to $[Cu_2(NO)O]^{2+}$ occurs via a rate-limiting reaction with NO and bypasses the dicopper oxo intermediate, a mechanism distinct from that of diFe-mediated NO reduction to N_2O.

INTRODUCTION

A crucial signaling molecule at the nanomolar level, nitric oxide (NO), is an acute toxin at high concentrations that participates in immune defense in mammals.[1,2] To detoxify excess nitric oxide, biology employs metalloenzymes to convert NO to N_2O through metal nitrosyl (typically Cu or Fe) intermediates.[3−8] Heme/non-heme,[9−17] heme/copper,[18−20] and flavo-diiron[21,22] NO reductases (NOR) are three classes of enzymes that contain bimetallic active sites capable of converting NO to N_2O. The mechanism of NO conversion to N_2O at bimetallic site often involves the coupling of adjacent metal nitrosyl species to afford metal hyponitrite ($^-O-N=N-O^-$) intermediates, which release N_2O and generate bimetallic μ-oxo species (M–O–M, M = Fe^{III} or Cu^{II}, Scheme 1A). Studies by Lehnert,[23−28] Kurtz,[21,29,30] Majumdar,[31,32] Goldberg,[33,34] and others[35,36] showed that reduction of NO at non-heme diiron centers can proceed through direct,[24,33] semireduced,[25,32] or super-reduced[31] mechanisms (Scheme 1B). Recently, Wade and Dincă reported Fe^{II}-based metal–organic frameworks (MOFs) that reduce NO to N_2O.[37,38]

Copper(I) complexes are known to promote NO disproportionation to afford N_2O and Cu^{II}-NO_2. Karlin reported that treatment of $(tmpa)Cu^{I}$ with NO generates N_2O through a fully characterized dicopper(II,II) *trans*-hyponitrite ($^-O-N=N-O^-$) intermediate (Scheme 1A).[39−41] In another example by Agapie,[42] a *trans*-hyponitrite intermediate was also isolated when tricopper(I) precursor was treated with excess NO. Apart from NO coupling at dicopper sites, Tolman,[43−45] Dincă,[46,47] and Warren[48] demonstrated the coupling of NO at mono-copper sites through putative

Scheme 1. $NO^{\bullet}$ Activation Pathways in Enzymes and Models

A *$NO^{\bullet}$ coupling through bimetallic hyponitrite intermediate*

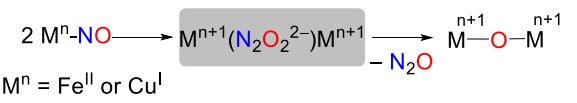

B *$NO^{\bullet}$ coupling through diiron dinitrosyl intermediate*

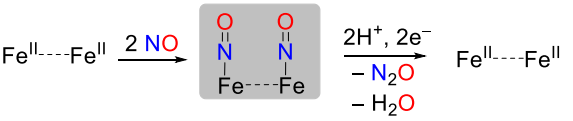

C *$NO^{\bullet}$ coupling through mononuclear hyponitrite intermediate*

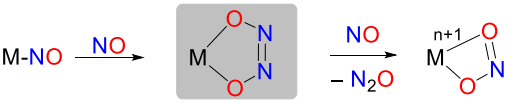

Received: September 8, 2022

mononuclear Cu *cis*-hyponitrite intermediates (Scheme 1C). Analogous NO coupling at mono-Ni center through hyponitrite has also been demonstrated.[49,50]

Despite these experimental and computation advancements,[51−53] the mechanistic picture of NO coupling is not complete, particularly regarding how the NO motif "flip" from N-bound nitrosyl to O-bound hyponitrite during the N═N bond formation step.[8,40] Additionally, the identity of the copper species after N_2O elimination is elusive. Although dicopper(II,II) oxo $[Cu_2O]^{2+}$ species is often proposed, its direct formation from dicopper (II,II) hyponitrite has yet to be confirmed. Instead, the formation of copper(II) nitrite is often observed, which involves the reaction with a third equivalent of NO.[40,43−45] The divergent products after N_2O elimination, i.e., diiron oxo vs copper nitrite, might have implications for why nature typically employs Fe(II) instead of Cu(I) for the conversion of NO to N_2O, albeit both appear to be efficient in synthetic systems.

Recently, our group characterized the dicopper intermediate before the formation of nitrite as a dicopper μ-oxo μ-nitrosyl species.[54−56] Reaction of three equivalents of NO with dicopper(I) Py_4DMB complex (Py_4DMB = 1,2-bis(di-(pyridin-2-yl)methoxy)benzene, **L**) affords N_2O (98% yield) and $[LCu^{II}Cu^{III}(\mu\text{-}O)(\mu\text{-}NO^-)]^{2+}$ (Scheme 2). The Cu(II), Cu(III), O^{2-}, and NO^- formula is based on the N═O stretching frequency at 1554 cm^{-1} and the four-line pattern of $S = 1/2$ EPR signal. The third equivalent of NO is trapped as a bridging NO^- between the two Cu centers, though it is unclear if binding of the third equivalent of NO occurs before or after the N_2O release (Scheme 2).

Scheme 2. NO• Coupling at Dicopper Dinitrosyl Diamond Core

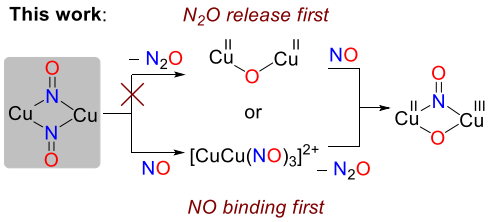

Notably, a green intermediate preceding the elimination of N_2O was observed; however, we did not assert what it might be. Further characterization of this intermediate will provide an opportunity to elucidate the mechanism by which predis-positioned dicopper centers promote NO reduction. Herein, we present the characterization of this green intermediate as an unprecedented $[Cu_2(NO)_2]^{2+}$ complex (Scheme 2, Enemark−Feltham notation $\{Cu_2(NO)_2\}^{22}$). Resonance Raman (rR) spectroscopic characterization of the $[Cu_2(NO)_2]^{2+}$ species suggests that it has a symmetric diamond-core structure with bis-μ-NO ligands. The 1:1 Cu/NO ratio was further confirmed by a series of NO trapping experiments. Mechanistic study indicates that the conversion of $[Cu_2(NO)_2]^{2+}$ to $[Cu_2(O)(NO)]^{2+}$ does not proceed through the commonly proposed $[Cu_2(O)]^{2+}$ species (Scheme 2).

RESULTS AND DISCUSSION

Synthesis of Dicopper Dinitrosyl Complex 2. Addition of excess NO to dicopper(I,I) Py_4DMB complex $[LCu_2^I(MeCN)_2][BAr_4^F]_2$ (**1**) at −40 °C in tetrahydrofuran (THF) generated $[LCu_2(\mu\text{-}O)(\mu\text{-}NO)]^{2+}$ complex (**3**)[54] through the intermediacy of green species **2** (Figure 1A). Complex **2** (λ = 625 nm, ε = 2300 $M^{-1}cm^{-1}$, Figure 1B) is stable at −95 °C and converts to **3** cleanly at −40 °C (Figure 1C). We could not obtain single crystals of **2** due to its thermal sensitivity. EPR analysis suggested that **2** is EPR-silent (Figures S38 and S39).

Given the ability of **2** to release N_2O, we hypothesized that it might be either a dicopper hyponitrite or a dicopper nitrosyl species. Due to thermal sensitivity, only a few copper hyponitrite[40−42,47,48] and copper nitrosyl complexes have

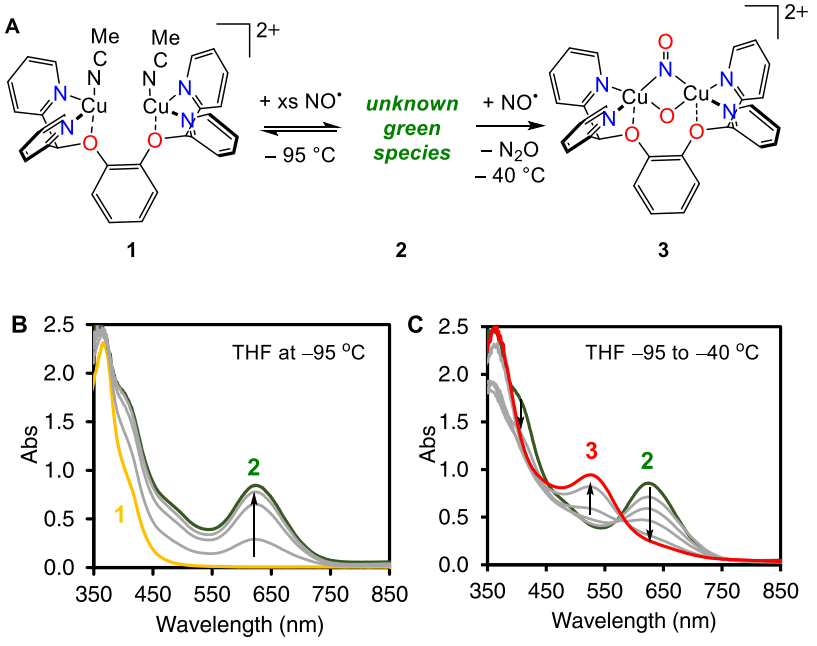

Figure 1. (A) Reaction scheme and (B) corresponding UV−vis spectra of the conversion of **1** to **2** at −95 °C, and (C) **2** to **3** from −95 to −40 °C in THF (0.39 mM).

https://doi.org/10.1021/jacs.2c09523
J. Am. Chem. Soc. XXXX, XXX, XXX−XXX

been characterized.[43,44,54−59] Considering literature precedence, we proposed several possible binding modes of NO: (i) dicopper (II,II) *trans*-hyponitrite, (ii) dicopper (II,II) *cis*-hyponitrite,[60] (iii) dicopper bis-μ-NO $[Cu_2(NO)_2]^{2+}$,[61] or (iv) dicopper mono-μ-NO $[Cu_2NO]^{2+}$ (Scheme 3).

Scheme 3. Potential Structures of 2

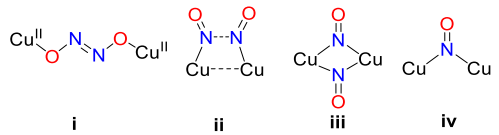

Resonance Raman Characterization of 2. The various possible binding modes of NO and hyponitrite can be differentiated by vibrational characterization of **2** using rR spectroscopy. To avoid thermal decomposition of **2** to **3** and overlapping solvent background peaks, rR samples of **2** were prepared in THF-d_8 using $^{14}NO/^{15}NO$ at −80 °C (see the Supporting Information). The rR spectra of **2** excited with 568 nm laser reveal three resonantly enhanced, ^{15}N isotopically sensitive peaks at 390.6, 414.1, and 1528 cm^{-1} (Figure 2A−D). The peak with the highest intensity at 1528 cm^{-1} has a 26 cm^{-1} isotopic shift, matching well with Hooke's law calculation for a $^{14/15}N{=}O$ oscillator. To ensure the 1528 cm^{-1} peak is not a result of **3** contamination (N═O IR-stretch at ca. 1554 cm^{-1}),[54] we also performed rR measurement with 514 nm laser, where **3** is more enhanced than **2**. The peak intensity of the 1528 cm^{-1} band diminished significantly with the 514 nm laser, suggesting the N═O peak at 1528 cm^{-1} derives from **2** (Figures S21 and 22). The two lower-frequency, ^{15}N isotopically sensitive peaks at 390.6 (−10) and 414.1 (−10) cm^{-1} were assigned to Cu−N-based vibrations.

Since we did not observe diagnostic isotopically sensitive peaks related to N−N, N═N, or N−O stretches,[42,47,48,62,63] dicopper(II,II) hyponitrite intermediates **i** and **ii** were ruled out. Both dicopper dinitrosyl diamond core $[Cu_2(\mu\text{-}NO)_2]^{2+}$ **iii** and dicopper mononitrosyl **iv** (Scheme 3) could be consistent with one set of N═O stretching bands. However, neither **iii** nor **iv** has been reported in the literature. Nonetheless, there are four reports of vibrational data for dicopper μ^2-N nitrosyl complexes at higher formal oxidation states: $[Cu^ICu^{II}(\mu\text{-}NO)]^{3+}$ (1670 cm^{-1}),[59] $[Cu^{II}Cu^{II}(\mu^2\text{-}NO^-)]^{3+}$ (1536[57] and 1567[55] cm^{-1}), and $[Cu^{II}Cu^{III}(\mu^2\text{-}O)(\mu^2\text{-}NO^-)]^{2+}$ (1554 cm^{-1}).[54] Additionally, the diiron dinitrosyl diamond-core complex $\{Fe_2(NO)_2\}^{16}$ reported by Lehnert exhibits a single IR-active N═O stretch at 1350 cm^{-1}.[61] Given the EPR-silent nature of **2**, it is more likely to be **iii** than **iv** (S = 1/2).

Computational Study. To aid in the interpretation of rR data, we calculated the vibrational frequencies using density functional theory with dispersion correction (B3LYP/6−311+G(d)/D3BJ). We considered dicopper dinitrosyl **iii**, dicopper mononitrosyl **iv**, as well as several alternative binding modes of $[LCu_2(NO)_2]^{2+}$ complex in singlet and triplet states (**v**, **vi**, Figure 3 top). The ground-state energies of most dicopper dinitrosyl species considered are within 6 kcal/mol (see Supporting Information Figure S29). Their structures and calculated Raman shifts are summarized in Figure 3 and Tables S2−S4. The optimized structure of dicopper dinitrosyl $[LCu_2(\mu^2\text{-}NO)_2]^{2+}$ complex (**iii**) at triplet S = 1 state shows a Raman-active N═O stretch at 1531 cm^{-1} and low-intensity Cu−N-based vibrations at 378.2 and 431.7 cm^{-1}. These values match the experimental rR stretches very well (1528, 390.6, 414.1 cm^{-1}). The calculated Raman stretches for other possible dicopper (di)nitrosyl species at the same level of theory do not match the experimental results (Figure 3).

To elucidate the electronic structure of **iii** in the triplet S = 1 state, we examined its frontier orbitals at B3LYP/6−311+G(d)/D3BJ level of theory. The two SOMOs of S = 1 **iii** are primarily based on two sets of orthogonal NO π^* orbitals (Figure 4). Ferromagnetic coupling between them

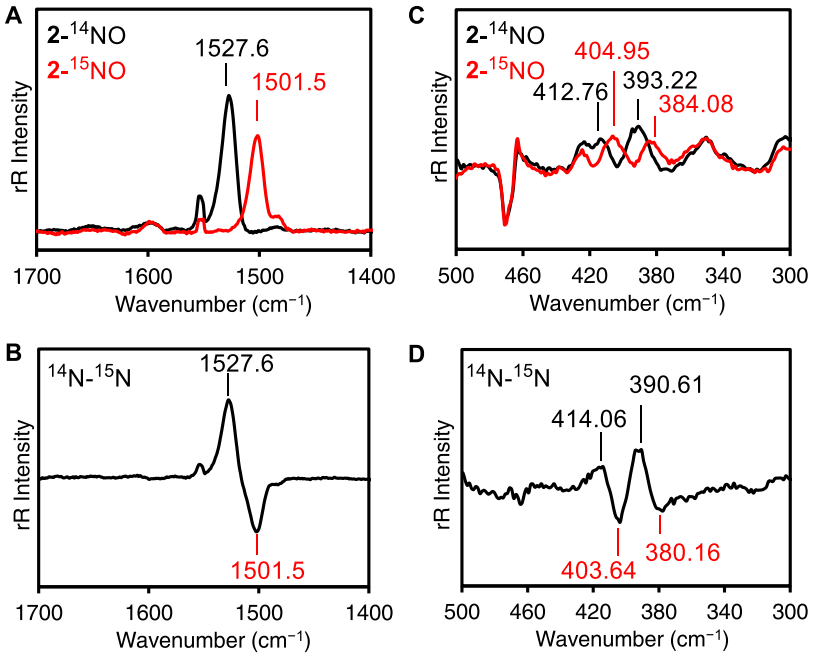

Figure 2. (A, C) Resonance Raman spectra of **2**-N^{15} (red) and **2**-N^{14} (black) collected with 568 nm excitation laser. (B, D) Differential spectra. Three ^{15}N isotopically sensitive peaks at 390.6(−10.4), 414.1 (−10.4), and 1528 (−26) cm^{-1} were observed.

https://doi.org/10.1021/jacs.2c09523
J. Am. Chem. Soc. XXXX, XXX, XXX−XXX

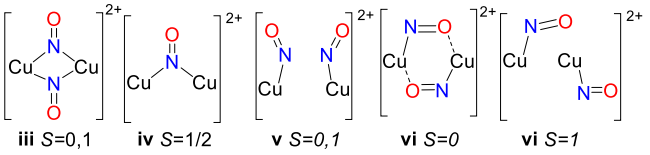

	N=O cm^{-1} (^{14}N–^{15}N shift)	Cu-N cm^{-1} (^{14}N–^{15}N shift)
iv *S*=1/2	1642.9 (29.0)	367.5 (7.2), 479.6 (14.8)
iii *S=0*	1714.3 (31.3)	428.7 (9.8), 582.7 (15.6)
iii *S=1*	1531.3 (25.2)	378.2 (8.3), 431.7 (8.2)
iii *S=0*[a]	1730.0 (31.5)	361.0 (7.3), 421.0 (11.2)
v *S=0*	1733.7 (30.9)	469.3 (12.7), 495.8 (14.0)
v *S=1*	1777.3 (32.1)	414.6 (8.4), 425.1 (10.6))
vi *S=0*	1700.2 (30.2)	524.4 (12.1), 492.2 (11.7)
vi *S=1*	1787.5 (32.5)	427.9 (11.3)
Exp	1527.6 (26.1)	390.6 (10.4), 414.1 (10.4)

Figure 3. Calculated structures of dicopper nitrosyl complexes and corresponding N═O and Cu−N stretching frequencies. [a]Open-shell singlet.

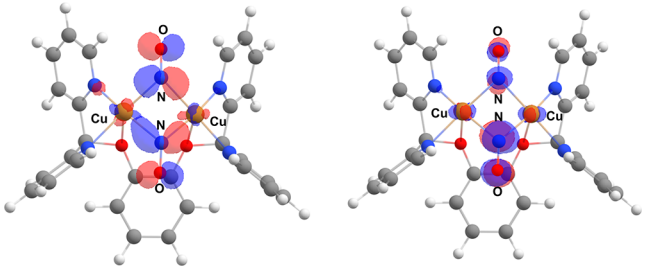

Figure 4. SOMOs of *S* = 1 dicopper dinitrosyl diamond-core complex.

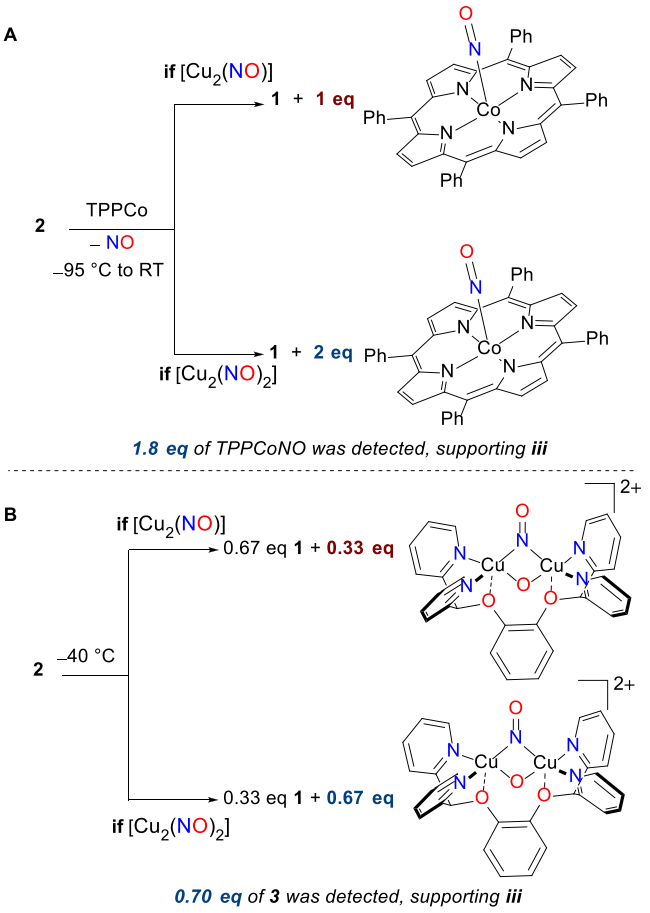

Figure 5. Determining the number of nitrosyl ligands in **2** by quantifying (A) the reversibly released NO$^{\bullet}$ (with TPPCo trapping) and (B) the conversion of **2** to **3**.

mediated by the Cu centers gives rise to the *S* = 1 spin state (see Figure S30 for spin density plot). Based on the calculated frontier orbitals (Figure S31), complex **2** is best described as two Cu^{I} centers with two bridging NO motifs, which is distinct from Lehnert's $\{Fe_2(NO)_2\}^{16}$ diamond-core complex that has two low-spin Fe^{II} centers and two bridging NO^{-} ligands.[61] We attribute this difference to the weaker back-bonding ability of Cu to NO π^* and the less reducing nature of Cu than Fe.

Reactivity of Dicopper Dinitrosyl Complex 2. The reactivity studies of **2** provided complementary information on the stoichiometry of Cu/NO in **2**. Considering the weak binding affinity of NO at **1**, we sought to quantify the NO released from **2** by trapping the evolved gas with cobalt(II) porphyrin (TPP)Co(II) (TPP = tetraphenylporphyrin) (Figure 5A).[56,64,65] The resulting $\{CoNO\}^8$ product can be quantified with ultraviolet−visible (UV−vis) and ^{1}H NMR spectroscopy. Complex **2** was first generated in situ by treating **1** with NO at −95 °C. The excess NO was carefully removed by purging the solution with a stream of N_2 gas before a solution of (TPP)Co(II) was added to the solution to capture NO released from **2**, as the solution warmed up to 20 °C gradually. The conversion of (TPP)Co^{II} to $\{CoNO\}^8$ was analyzed via UV−vis and quantitative ^{1}H NMR, showing the release of 1.8(1) eq of NO per **1** (90% yield) consistent with a 1:1 stoichiometry of Cu/NO (Figures S11−S16). Importantly, control experiments performed under identical NO addition, purging, and trapping conditions in the absence of complex **1** showed less than 0.14 eq $\{CoNO\}^8$ formation. This NO trapping experiment supports the assignment of **2** as **iii** instead of **iv** since dicopper mononitrosyl **iv** could only release up to 1 eq of NO.

Further evidence for the assignment of **2** as $[Cu_2(NO)_2]^{2+}$ was obtained by studying the conversion of **2** to **3**. Considering that the formation of each equivalent of **3** requires three equivalents of NO per dicopper complex, a NO-free solution of **2** should afford 2/3 eq (67%) of **3**, leaving behind 1/3 eq of unreacted **1**. Indeed, warming up a NO-free solution of **2** at −40 °C cleanly afforded **3** in 70% yield, consistent with the assignment of **2** as dicopper dinitrosyl **iii** (Figure 5B).

Kinetics of N_2O Release from 2 in the Presence of NO. After establishing the green intermediate **2** as the dicopper dinitrosyl species, we investigated the mechanism of N_2O release by monitoring the kinetics of the conversion of **2** to **3** under different concentrations of NO. Since no intermediate was observed during the conversion of **2** to **3**, it is reasonable to assume that the first kinetic step, either the release of N_2O or binding of NO, is rate-limiting. Therefore, there are two mechanistic possibilities. First, complex **2** could release N_2O in a rate-limiting step to generate a putative dicopper (II,II) oxo species that quickly captures another equivalent of NO to afford **3** (mechanism A, Figure 6A). Alternatively, complex **2** can react with another equivalent of NO in a rate-limiting step to release N_2O and afford **3** in a kinetically invisible step via a $[Cu_2(NO)_3]^{2+}$-type of intermediates or transition states

https://doi.org/10.1021/jacs.2c09523
J. Am. Chem. Soc. XXXX, XXX, XXX−XXX

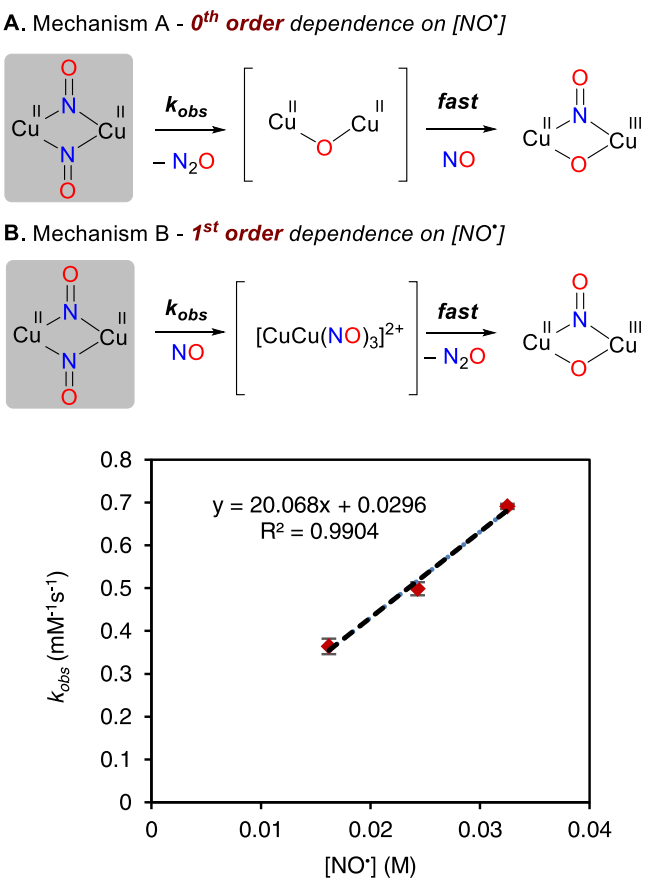

Figure 6. (A) Two mechanistic possibilities for the conversion of **2** to **3**. (B) Plot of k_{obs} of the conversion of **2** to **3** at −40 °C vs [NO] indicates first-order dependency on [NO], supporting mechanism B.

(mechanism B, Figure 6B).[8,48,66] These two scenarios differ in the kinetic dependence on NO concentration. Therefore, they may be distinguished by measuring k_{obs} as a function of [NO].

The rate of conversion of **2** to **3** was monitored by UV−vis spectroscopy at three NO concentrations at −40 °C. Generally, the decay rate of **2** matches the formation rate of **3** within experimental error (Figure S27). The rate constant k_{obs} was determined by kinetic simulation with KinTek software. Due to the solubility of NO in the solution, we can only measure k_{obs} at three different NO concentrations. A plot of k_{obs} vs [NO] reveals a linear relationship (R^2 = 0.99) with an intercept close to 0, suggesting a first-order dependency on NO concentration. This kinetic analysis argues against the commonly proposed mechanism A, where complex **2** releases N_2O directly to afford dicopper oxo species.[53] Instead, the binding of a third equivalent of NO at **2** is necessary to promote the formation of N═N bond (Figure 6B).

Plausible Mechanisms of N_2O Formation. A plausible mechanism for N_2O formation involves the binding of the third equivalent of NO on the top of the dicopper dinitrosyl diamond core to form an ON···N−O···NO ligand (Figure 7A). Cleavage of N−O bond leads to the formation of N_2O and NO_2^-, as shown by the computational study by Metz and others.[51] The direct capture of NO by the dinitrosyl moiety may be guided by the orbital interaction of NO π^* with the SOMO of **2** perpendicular to the plane of the $[Cu_2(NO)_2]$-diamond core (Figure 4, right). In this mechanistic scenario, the NO does not need to "flip" to an O-bound mode to form a hyponitrite intermediate.

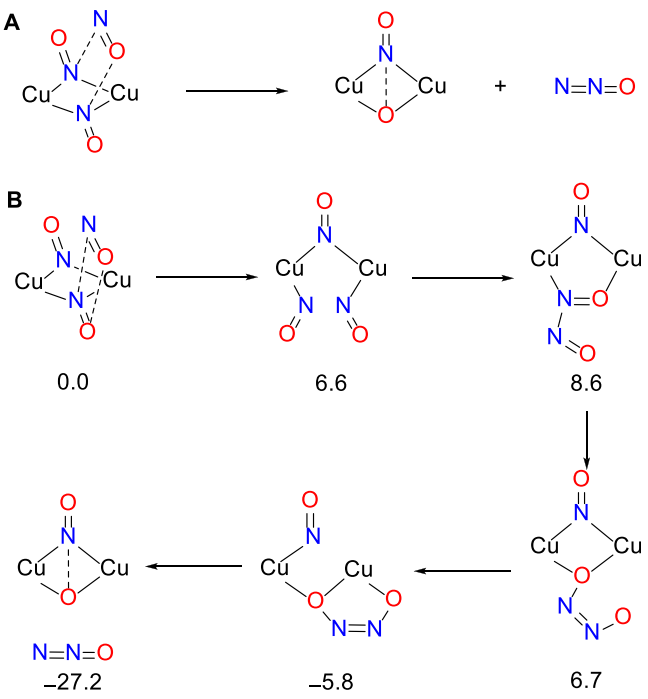

Figure 7. Two plausible pathways for N_2O release and the relative computed free energies (kcal/mol) at the B3LYP/6-311+G(d)/D3BJ level of theory.

Alternatively, binding of the third equivalent of NO can result in a number of dicopper nitrosyl hyponitrite complexes (Figure 7B, more possible structures are shown in Figure S37), which release N_2O spontaneously, as shown by Karlin et al.[40,41] Figure 7B illustrates one of many possible pathways for the isomerization of trinitrosyl complexes to hyponitrite. Density functional theory (DFT) calculations performed at the UB3LYP/6-311+G(d)_D3BJ level of theory suggests that isomerization of hyponitrite at dicopper center to O-bound form is possible, consistent with the findings by Lehnert et al.[52]

CONCLUSIONS

In summary, we have characterized the first example of a diamond core $[Cu_2(NO)_2]^{2+}$ complex. Resonance Raman characterization, in conjunction with DFT calculations, suggests that this compound is best described as having two Cu^I centers with two bridging NO ligands. The reactivity study firmly established the 1:1 ratio of Cu/NO in $[Cu_2(NO)_2]^{2+}$ complex. The release of N_2O from $[Cu_2(NO)_2]^{2+}$ complex involves the reaction with a third equivalent of NO and does not proceed through the commonly proposed $[Cu_2(O)]^{2+}$ species.

While Fe(II) and Cu(I) are both effective in the reductive coupling of NO to N_2O, the fates of the O atoms generated from these two processes are different. Fe enzymes dispose of the O atom as H_2O, while Cu complexes generate NO_2^-. Our study provides a potential explanation for the divergent products of NO reduction at Fe and Cu. We showed that N_2O was released from $[LCu_2(NO)_2]^{2+}$ after the binding of the third equivalent of NO. This process bypasses $[LCu_2O]^{2+}$ to afford $[LCu_2(NO)O]^{2+}$ species, which is poised for nitrite formation. The mechanistic difference between Cu and Fe might have implications on why pathogens choose Fe instead of Cu enzymes for NO reduction, as high concentrations of nitrite can be toxic to pathogens. Finally, our study suggests

https://doi.org/10.1021/jacs.2c09523
J. Am. Chem. Soc. XXXX, XXX, XXX−XXX

that $[Cu_2(NO)O]^{2+}$ should be considered as an intermediate in systems where $[Cu_2O]^{2+}$ is proposed as the active species, e.g., catalytic NO_x decomposition at Cu-exchanged zeolite[67,68] and nitrite-driven anaerobic methane oxidation.[69−72] Ongoing work in our laboratory focuses on comparing the reactivity profiles of $[Cu_2(NO)O]^{2+}$ vs $[Cu_2O]^{2+}$.

■ ASSOCIATED CONTENT

Supporting Information

The Supporting Information is available free of charge at https://pubs.acs.org/doi/10.1021/jacs.2c09523.

Experimental details, including characterization data, spectra, kinetic data, computational procedures, and results (PDF)

■ AUTHOR INFORMATION

Corresponding Authors

Hannah S. Shafaat − *Department of Chemistry & Biochemistry, The Ohio State University, Columbus, Ohio 43210, United States*; Email: shafaat.1@osu.edu

Shiyu Zhang − *Department of Chemistry & Biochemistry, The Ohio State University, Columbus, Ohio 43210, United States*; Email: zhang.8941@osu.edu

Authors

Wenjie Tao − *Department of Chemistry & Biochemistry, The Ohio State University, Columbus, Ohio 43210, United States*

Samantha Carter − *Department of Chemistry & Biochemistry, The Ohio State University, Columbus, Ohio 43210, United States*

Regina Trevino − *Department of Chemistry & Biochemistry, The Ohio State University, Columbus, Ohio 43210, United States*

Weiyao Zhang − *Department of Chemistry & Biochemistry, The Ohio State University, Columbus, Ohio 43210, United States*

Complete contact information is available at: https://pubs.acs.org/10.1021/jacs.2c09523

Notes

The authors declare no competing financial interest.

■ ACKNOWLEDGMENTS

This material is based on work supported by the U.S. National Science Foundation under award no. CHE-1904560 (S.Z.) and CHE-1454289/CHE-2108684 (H.S.S). The authors thank The Ohio State University Department of Chemistry and Biochemistry for additional financial support. High-performance computing resources were provided by the Ohio Supercomputer Center.

■ REFERENCES

(1) Bogdan, C. Nitric Oxide and the Immune Response - Nature Immunology. *Nat. Immunol.* **2001**, *2*, 907−916.

(2) Sarti, P.; Fiori, P. L.; Forte, E.; Rappelli, P.; Teixeira, M.; Mastronicola, D.; Sanciu, G.; Giuffré, A.; Brunori, M. Trichomonas Vaginalis Degrades Nitric Oxide and Expresses a Flavorubredoxin-like Protein: A New Pathogenic Mechanism? *Cell. Mol. Life Sci.* **2004**, *61*, 618−623.

(3) Wasser, I. M.; de Vries, S.; Moënne-Loccoz, P.; Schröder, I.; Karlin, K. D. Nitric Oxide in Biological Denitrification: Fe/Cu Metalloenzyme and Metal Complex NOx Redox Chemistry. *Chem. Rev.* **2002**, *102*, 1201−1234.

(4) Moënne-Loccoz, P. Spectroscopic Characterization of Heme Iron-Nitrosyl Species and Their Role in NO Reductase Mechanisms in Diiron Proteins. *Nat. Prod. Rep.* **2007**, *24*, 610−620.

(5) Schopfer, M. P.; Wang, J.; Karlin, K. D. Bioinspired Heme, Heme/Nonheme Diiron, Heme/Copper, and Inorganic NOx Chemistry: ·NO (g) Oxidation, Peroxynitrite-Metal Chemistry, and ·NO (g) Reductive Coupling. *Inorg. Chem.* **2010**, *49*, 6267−6282.

(6) Liu, J.; Chakraborty, S.; Hosseinzadeh, P.; Yu, Y.; Tian, S.; Petrik, I.; Bhagi, A.; Lu, Y. Metalloproteins Containing Cytochrome, Iron-Sulfur, or Copper Redox Centers. *Chem. Rev.* **2014**, *114*, 4366−4369.

(7) Ferousi, C.; Majer, S. H.; Dimucci, I. M.; Lancaster, K. M. Biological and Bioinspired Inorganic N-N Bond-Forming Reactions. *Chem. Rev.* **2020**, *120*, 5252−5307.

(8) Lehnert, N.; Kim, E.; Dong, H. T.; Harland, J. B.; Hunt, A. P.; Manickas, E. C.; Oakley, K. M.; Pham, J.; Reed, G. C.; Alfaro, V. S. The Biologically Relevant Coordination Chemistry of Iron and Nitric Oxide: Electronic Structure and Reactivity. *Chem. Rev.* **2021**, *121*, 14682−14905.

(9) Hendriks, J.; Warne, A.; Gohlke, U.; Haltia, T.; Ludovici, C.; Lübben, M.; Saraste, M. The Active Site of the Bacterial Nitric Oxide Reductase Is a Dinuclear Iron Center. *Biochemistry* **1998**, *37*, 13102−13109.

(10) Moënne-Loccoz, P.; de Vries, S. Structural Characterization of the Catalytic High-Spin Heme b of Nitric Oxide Reductase: A Resonance Raman Study. *J. Am. Chem. Soc.* **1998**, *120*, 5147−5152.

(11) Moënne-Loccoz, P.; Richter, O. M. H.; Huang, H. W.; Wasser, I. M.; Ghiladi, R. A.; Karlin, K. D.; de Vries, S. Nitric Oxide Reductase from *Paracoccus denitrificans* Contains an Oxo-Bridged Heme/Non-Heme Diiron Center. *J. Am. Chem. Soc.* **2000**, *122*, 9344−9345.

(12) Lu, S.; Suharti; de Vries, S.; Moënne-Loccoz, P. Two CO Molecules Can Bind Concomitantly at the Diiron Site of NO Reductase from *Bacillus azotoformans*. *J. Am. Chem. Soc.* **2004**, *126*, 15332−15333.

(13) Kumita, H.; Matsuura, K.; Hino, T.; Takahashi, S.; Hori, H.; Fukumori, Y.; Morishima, I.; Shiro, Y. NO Reduction by Nitric-Oxide Reductase from Denitrifying Bacterium *Pseudomonas aeruginosa*: Characterization of Reaction Intermediates That Appear in the Single Turnover Cycle. *J. Biol. Chem.* **2004**, *279*, 55247−55254.

(14) Yeung, N.; Lin, Y. W.; Gao, Y. G.; Zhao, X.; Russell, B. S.; Lei, L.; Miner, K. D.; Robinson, H.; Lu, Y. Rational Design of a Structural and Functional Nitric Oxide Reductase. *Nature* **2009**, *462*, 1079−1082.

(15) Lu, Y.; Yeung, N.; Sieracki, N.; Marshall, N. M. Design of Functional Metalloproteins. *Nature* **2009**, *460*, 855−862.

(16) Hino, T.; Matsumoto, Y.; Nagano, S.; Sugimoto, H.; Fukumori, Y.; Murata, T.; Iwata, S.; Shiro, Y. Structural Basis of Biological N2O Generation by Bacterial Nitric Oxide Reductase. *Science* **2010**, *330*, 1666−1670.

(17) Collman, J. P.; Yang, Y.; Dey, A.; Decréau, R. A.; Ghosh, S.; Ohta, T.; Solomon, E. I. A Functional Nitric Oxide Reductase Model. *Proc. Natl. Acad. Sci. U.S.A.* **2008**, *105*, 15660−15665.

(18) Wang, J.; Schopfer, M. P.; Sarjeant, A. A. N.; Karlin, K. D. Heme-Copper Assembly Mediated Reductive Coupling of Nitrogen Monoxide(·NO). *J. Am. Chem. Soc.* **2009**, *131*, 450−451.

(19) Varotsis, C.; Ohta, T.; Kitagawa, T.; Soulimane, T.; Pinakoulaki, E. The Structure of the Hyponitrite Species in a Heme Fe-Cu Binuclear Center. *Angew. Chem., Int. Ed.* **2007**, *46*, 2210−2214.

(20) Zhao, X.; Yeung, N.; Russell, B. S.; Garner, D. K.; Lu, Y. Catalytic Reduction of NO to N_2O by a Designed Heme Copper Center in Myoglobin: Implications for the Role of Metal Ions. *J. Am. Chem. Soc.* **2006**, *128*, 6766−6767.

(21) Weitz, A. C.; Giri, N.; Caranto, J. D.; Kurtz, D. M.; Bominaar, E. L.; Hendrich, M. P. Spectroscopy and DFT Calculations of a Flavo-Diiron Enzyme Implicate New Diiron Site Structures. *J. Am. Chem. Soc.* **2017**, *139*, 12009−12019.

(22) Silaghi-Dumitrescu, R.; Kurtz, D. M.; Ljungdahl, L. G.; Lanzilotta, W. N. X-Ray Crystal Structures of Moorella Thermoacetica FprA. Novel Diiron Site Structure and Mechanistic Insights into a

Scavenging Nitric Oxide Reductase. *Biochemistry* **2005**, *44*, 6492−6501.
(23) Zheng, S.; Berto, T. C.; Dahl, E. W.; Hoffman, M. B.; Speelman, A. L.; Lehnert, N. The Functional Model Complex $[Fe_2(BPMP)(OPr)(NO)_2](BPh_4)_2$ Provides Insight into the Mechanism of Flavodiiron NO Reductases. *J. Am. Chem. Soc.* **2013**, *135*, 4902−4905.
(24) Dong, H. T.; White, C. J.; Zhang, B.; Krebs, C.; Lehnert, N. Non-Heme Diiron Model Complexes Can Mediate Direct NO Reduction: Mechanistic Insight into Flavodiiron NO Reductases. *J. Am. Chem. Soc.* **2018**, *140*, 13429−13440.
(25) White, C. J.; Speelman, A. L.; Kupper, C.; Demeshko, S.; Meyer, F.; Shanahan, J. P.; Alp, E. E.; Hu, M.; Zhao, J.; Lehnert, N. The Semireduced Mechanism for Nitric Oxide Reduction by Non-Heme Diiron Complexes: Modeling Flavodiiron Nitric Oxide Reductases. *J. Am. Chem. Soc.* **2018**, *140*, 2562−2574.
(26) Dong, H. T.; Camarena, S.; Sil, D.; Lengel, M. O.; Zhao, J.; Hu, M. Y.; Alp, E. E.; Krebs, C.; Lehnert, N. What Is the Right Level of Activation of a High-Spin $\{FeNO\}^7$ Complex to Enable Direct N−N Coupling? Mechanistic Insight into Flavodiiron NO Reductases. *J. Am. Chem. Soc.* **2022**, *144*, 16395−16409.
(27) White, C. J.; Lengel, M. O.; Bracken, A. J.; Kampf, J. W.; Speelman, A. L.; Alp, E. E.; Hu, M. Y.; Zhao, J.; Lehnert, N. Distortion of the $[FeNO]_2$ Core in Flavodiiron Nitric Oxide Reductase Models Inhibits N-N Bond Formation and Promotes Formation of Unusual Dinitrosyl Iron Complexes: Implications for Catalysis and Reactivity. *J. Am. Chem. Soc.* **2022**, *144*, 3804−3820.
(28) Dong, H. T.; Zong, Y.; Bracken, A. J.; Lengel, M. O.; Kampf, J. W.; Sil, D.; Krebs, C.; Lehnert, N. Synthesis and Characterization of a Model Complex for Flavodiiron NO Reductases That Stabilizes a Diiron Mononitrosyl Complex. *J. Inorg. Biochem.* **2022**, *229*, 111723−111726.
(29) Caranto, J. D.; Weitz, A.; Hendrich, M. P.; Kurtz, D. M. The Nitric Oxide Reductase Mechanism of a Flavo-Diiron Protein: Identification of Active-Site Intermediates and Products. *J. Am. Chem. Soc.* **2014**, *136*, 7981−7992.
(30) Weitz, A. C.; Giri, N.; Frederick, R. E.; Kurtz, D. M.; Bominaar, E. L.; Hendrich, M. P. Spectroscopy and DFT Calculations of Flavo-Diiron Nitric Oxide Reductase Identify Bridging Structures of NO-Coordinated Diiron Intermediates. *ACS Catal.* **2018**, *8*, 11704−11715.
(31) Jana, M.; Pal, N.; White, C. J.; Kupper, C.; Meyer, F.; Lehnert, N.; Majumdar, A. Functional Mononitrosyl Diiron(II) Complex Mediates the Reduction of NO to N_2O with Relevance for Flavodiiron NO Reductases. *J. Am. Chem. Soc.* **2017**, *139*, 14380−14383.
(32) Jana, M.; White, C. J.; Pal, N.; Demeshko, S.; Cordes, C.; Meyer, F.; Lehnert, N.; Majumdar, A. Functional Models for the Mono- And Dinitrosyl Intermediates of FNORs: Semireduction versus Superreduction of NO. *J. Am. Chem. Soc.* **2020**, *142*, 6600−6616.
(33) Dey, A.; Gordon, J. B.; Albert, T.; Sabuncu, S.; Siegler, M. A.; MacMillan, S. N.; Lancaster, K. M.; Moënne-Loccoz, P.; Goldberg, D. P. A Nonheme Mononuclear $\{FeNO\}^7$ Complex That Produces N2O in the Absence of an Exogenous Reductant. *Angew. Chem., Int. Ed.* **2021**, *60*, 21558−21564.
(34) Confer, A. M.; McQuilken, A. C.; Matsumura, H.; Moënne-Loccoz, P.; Goldberg, D. P. A Nonheme, High-Spin $\{FeNO\}^8$ Complex That Spontaneously Generates N_2O. *J. Am. Chem. Soc.* **2017**, *139*, 10621−10624.
(35) Feig, A. L.; Bautista, M. T.; Lippard, S. J. A Carboxylate-Bridged Non-Heme Diiron Dinitrosyl Complex. *Inorg. Chem.* **1996**, *35*, 6892−6898.
(36) Lu, J.; Bi, B.; Lai, W.; Chen, H. Origin of Nitric Oxide Reduction Activity in Flavo−Diiron NO Reductase: Key Roles of the Second Coordination Sphere. *Angew. Chem., Int. Ed.* **2019**, *58*, 3795−3799.
(37) Brozek, C. K.; Miller, J. T.; Stoian, S. A.; Dinca, M. NO Disproportionation at a Mononuclear Site-Isolated Fe2+ Center in Fe^{2+}-MOF-5. *J. Am. Chem. Soc.* **2015**, *137*, 7495−7501.
(38) Cai, Z.; Tao, W.; Moore, C. E.; Zhang, S.; Wade, C. R. Direct NO Reduction by a Biomimetic Iron(II) Pyrazolate MOF. *Angew. Chem., Int. Ed.* **2021**, *60*, 21221−21225.
(39) Paul, P. P.; Karlin, K. D. Functional Modeling of Copper Nitrite Reductases: Reactions of NO_2^- or NO with Copper(I) Complexes. *J. Am. Chem. Soc.* **1991**, *113*, 6331−6332.
(40) Wijeratne, G. B.; Hematian, S.; Siegler, M. A.; Karlin, K. D. Copper(I)/NO(g) Reductive Coupling Producing a Trans-Hyponitrite Bridged Dicopper(II) Complex: Redox Reversal Giving Copper(I)/NO(g) Disproportionation. *J. Am. Chem. Soc.* **2017**, *139*, 13276−13279.
(41) Wijeratne, G. B.; Bhadra, M.; Siegler, M. A.; Karlin, K. D. Copper(I) Complex Mediated Nitric Oxide Reductive Coupling: Ligand Hydrogen Bonding Derived Proton Transfer Promotes N_2O(g) Release. *J. Am. Chem. Soc.* **2019**, *141*, 17962−17967.
(42) Lionetti, D.; de Ruiter, G.; Agapie, T. A Trans-Hyponitrite Intermediate in the Reductive Coupling and Deoxygenation of Nitric Oxide by a Tricopper-Lewis Acid Complex. *J. Am. Chem. Soc.* **2016**, *138*, 5008−5011.
(43) Carrier, S. M.; Ruggiero, C. E.; Tolman, W. B.; Jameson, G. B. Synthesis and Structural Characterization of a Mononuclear Copper Nitrosyl Complex. *J. Am. Chem. Soc.* **1992**, *114*, 4407−4408.
(44) Ruggiero, C. E.; Carrier, S. M.; Cramer, C. J.; Tolman, W. B.; Antholine, W. E.; Whittaker, J. W. Synthesis and Structural and Spectroscopic Characterization of Mononuclear Copper Nitrosyl Complexes: Models for Nitric Oxide Adducts of Copper Proteins and Copper-Exchanged Zeolites. *J. Am. Chem. Soc.* **1993**, *115*, 11285−11298.
(45) Schneider, J. L.; Carrier, S. M.; Ruggiero, C. E.; Young, V. G.; Tolman, W. B. Influences of Ligand Environment on the Spectroscopic Properties and Disproportionation Reactivity of Copper-Nitrosyl Complexes. *J. Am. Chem. Soc.* **1998**, *120*, 11408−11418.
(46) Wright, A. M.; Sun, C.; Dincă, M. Thermal Cycling of a MOF-Based NO Disproportionation Catalyst. *J. Am. Chem. Soc.* **2021**, *143*, 681−686.
(47) Sun, C.; Yang, L.; Ortuño, M. A.; Wright, A. M.; Chen, T.; Head, A. R.; López, N.; Dincă, M. Spectroscopic Evidence of Hyponitrite Radical Intermediate in NO Disproportionation at a MOF-Supported Mononuclear Copper Site. *Angew. Chem., Int. Ed.* **2021**, *60*, 7845−7850.
(48) Ghosh, P.; Stauffer, M.; Hosseininasab, V.; Kundu, S.; Bertke, J. A.; Cundari, T. R.; Warren, T. H. NO Coupling at Copper to Cis-Hyponitrite: N_2O Formation via Protonation and H-Atom Transfer. *J. Am. Chem. Soc.* **2022**, *144*, 15093−15099.
(49) Kundu, S.; Phu, P. N.; Ghosh, P.; Kozimor, S. A.; Bertke, J. A.; Stieber, S. C. E.; Warren, T. H. Nitrosyl Linkage Isomers: NO Coupling to N_2O at a Mononuclear Site. *J. Am. Chem. Soc.* **2019**, *141*, 1415−1419.
(50) Stredansky, M.; Moro, S.; Corva, M.; Sturmeit, H.; Mischke, V.; Janas, D.; Cojocariu, I.; Jugovac, M.; Cossaro, A.; Verdini, A.; Floreano, L.; Feng, Z.; Sala, A.; Comelli, G.; Windischbacher, A.; Puschnig, P.; Hohner, C.; Kettner, M.; Libuda, J.; Cinchetti, M.; Schneider, C. M.; Feyer, V.; Vesselli, E.; Zamborlini, G. Disproportionation of Nitric Oxide at a Surface-Bound Nickel Porphyrinoid. *Angew. Chem., Int. Ed.* **2022**, *61*, No. e202201916.
(51) Metz, S. N2O Formation via Reductive Disproportionation of NO by Mononuclear Copper Complexes: A Mechanistic DFT Study. *Inorg. Chem.* **2017**, *56*, 3820−3833.
(52) Van Stappen, C.; Lehnert, N. Mechanism of N-N Bond Formation by Transition Metal-Nitrosyl Complexes: Modeling Flavodiiron Nitric Oxide Reductases. *Inorg. Chem.* **2018**, *57*, 4252−4269.
(53) Kametani, Y.; Abe, T.; Yoshizawa, K.; Shiota, Y. Mechanistic Study on Reduction of Nitric Oxide to Nitrous Oxide Using a Dicopper Complex. *Dalton Trans.* **2022**, *51*, 5399−5403.

https://doi.org/10.1021/jacs.2c09523
J. Am. Chem. Soc. XXXX, XXX, XXX−XXX

(54) Tao, W.; Bower, J. K.; Moore, C. E.; Zhang, S. Dicopper M-oxo, M-nitrosyl Complex from the Activation of NO or Nitrite at a Dicopper Center. *J. Am. Chem. Soc.* **2019**, *141*, 10159−10164.
(55) Tao, W.; Moore, C. E.; Zhang, S. Redox-Neutral S-Nitrosation Mediated by a Dicopper Center. *Angew. Chem., Int. Ed.* **2021**, *60*, 15980−15987.
(56) Tao, W.; Yerbulekova, A.; Moore, C. E.; Shafaat, H. S.; Zhang, S. Controlling the Direction of S-Nitrosation versus Denitrosation: Reversible Cleavage and Formation of an S−N Bond within a Dicopper Center. *J. Am. Chem. Soc.* **2022**, *144*, 2867−2872.
(57) Paul, P. P.; Tyeklar, Z.; Farooq, A.; Karlin, K. D.; Liu, S.; Zubieta, J. Isolation and X-Ray Structure of a Dinuclear Copper-Nitrosyl Complex. *J. Am. Chem. Soc.* **1990**, *112*, 2430−2432.
(58) Fujisawa, K.; Tateda, A.; Miyashita, Y.; Okamoto, K. I.; Paulat, F.; Praneeth, V. K. K.; Merkle, A.; Lehnert, N. Structural and Spectroscopic Characterization of Mononuclear Copper(I) Nitrosyl Complexes: End-on versus Side-on Coordination of NO to Copper(I). *J. Am. Chem. Soc.* **2008**, *130*, 1205−1213.
(59) Cao, R.; Elrod, L. T.; Lehane, R. L.; Kim, E.; Karlin, K. D. A Peroxynitrite Dicopper Complex: Formation via Cu-NO and Cu-O2 Intermediates and Reactivity via O-O Cleavage Chemistry. *J. Am. Chem. Soc.* **2016**, *138*, 16148−16158.
(60) Arikawa, Y.; Asayama, T.; Moriguchi, Y.; Agari, S.; Onishi, M. Reversible N−N Coupling of NO Ligands on Dinuclear Ruthenium Complexes and Subsequent N_2O Evolution: Relevance to Nitric Oxide Reductase. *J. Am. Chem. Soc.* **2007**, *129*, 14160−14161.
(61) Dong, H. T.; Speelman, A. L.; Kozemchak, C. E.; Sil, D.; Krebs, C.; Lehnert, N. The $Fe_2(NO)_2$ Diamond Core: A Unique Structural Motif In Non-Heme Iron−NO Chemistry. *Angew. Chem., Int. Ed.* **2019**, *58*, 17695−17699.
(62) Xu, N.; Campbell, A. L. O.; Powell, D. R.; Khandogin, J.; Richter-Addo, G. B. A Stable Hyponitrite-Bridged Iron Porphyrin Complex. *J. Am. Chem. Soc.* **2009**, *131*, 2460−2461.
(63) Arikawa, Y.; Onishi, M. Reductive N-N Coupling of NO Molecules on Transition Metal Complexes Leading to N_2O. *Coord. Chem. Rev.* **2012**, *256*, 468−478.
(64) Laverman, L. E.; Ford, P. C. Mechanistic Studies of Nitric Oxide Reactions with Water Soluble Iron(II), Cobalt(II), and Iron(III) Porphyrin Complexes in Aqueous Solutions: Implications for Biological Activity. *J. Am. Chem. Soc.* **2001**, *123*, 11614−11622.
(65) Richter-Addo, G. B.; Hodge, S. J.; Yi, G.-B.; Khan, M. A.; Ma, T.; Van Caemelbecke, E.; Guo, N.; Kadish, K. M. Synthesis, Characterization, and Spectroelectrochemistry of Cobalt Porphyrins Containing Axially Bound Nitric Oxide. *Inorg. Chem* **1996**, *35*, 6530−6538.
(66) Beagan, D. M.; Cabelof, A. C.; Pink, M.; Carta, V.; Gao, X.; Caulton, K. G. Nickel-Mediated N-N Bond Formation and N2O Liberation via Nitrogen Oxyanion Reduction. *Chem. Sci.* **2021**, *12*, 10664−10672.
(67) Gao, F.; Mei, D.; Wang, Y.; Szanyi, J.; Peden, C. H. F. Selective Catalytic Reduction over Cu/SSZ-13: Linking Homo- and Heterogeneous Catalysis. *J. Am. Chem. Soc.* **2017**, *139*, 4935−4942.
(68) Kwak, J. H.; Tran, D.; Szanyi, J.; Peden, C. H. F.; Lee, J. H. The Effect of Copper Loading on the Selective Catalytic Reduction of Nitric Oxide by Ammonia over Cu-SSZ-13. *Catal. Lett.* **2012**, *142*, 295−301.
(69) Ettwig, K. F.; Butler, M. K.; Le Paslier, D.; Pelletier, E.; Mangenot, S.; Kuypers, M. M. M.; Schreiber, F.; Dutilh, B. E.; Zedelius, J.; de Beer, D.; Gloerich, J.; Wessels, H. J. C. T.; van Alen, T.; Luesken, F.; Wu, M. L.; van de Pas-Schoonen, K. T.; Op den Camp, H. J. M.; Janssen-Megens, E. M.; Francoijs, K.-J.; Stunnenberg, H.; Weissenbach, J.; Jetten, M. S. M.; Strous, M. Nitrite-Driven Anaerobic Methane Oxidation by Oxygenic Bacteria. *Nature* **2010**, *464*, 543−548.
(70) Hu, B.-l.; Shen, L.-d.; Lian, X.; Zhu, Q.; Liu, S.; Huang, Q.; He, Z.-f.; Geng, S.; Cheng, D.-q.; Lou, L.-p.; Xu, X.-y.; Zheng, P.; He, Y.-f. Evidence for Nitrite-Dependent Anaerobic Methane Oxidation as a Previously Overlooked Microbial Methane Sink in Wetlands. *Proc. Natl. Acad. Sci. U.S.A.* **2014**, *111*, 4495−4500.
(71) Ettwig, K. F.; Shima, S.; Van De Pas-Schoonen, K. T.; Kahnt, J.; Medema, M. H.; Den Camp, H. J. M. O.; Jetten, M. S. M.; Strous, M. Denitrifying Bacteria Anaerobically Oxidize Methane in the Absence of Archaea. *Environ. Microbiol.* **2008**, *10*, 3164−3173.
(72) Francis, C. A.; Beman, J. M.; Kuypers, M. M. M. New Processes and Players in the Nitrogen Cycle: The Microbial Ecology of Anaerobic and Archaeal Ammonia Oxidation. *ISME J.* **2007**, *1*, 19−27.

https://doi.org/10.1021/jacs.2c09523
J. Am. Chem. Soc. XXXX, XXX, XXX−XXX